

The Velocities of Modern Horizontal Movements of Earth Crust in the South Sector of Yenisei Ridge According to GNSS Observations

Academician A. D. Gvishiani^{a,b}, V. N. Tatarinov^{a,b}, V. I. Kaftan^a, A. I. Manevich^{a,c*},
B. A. Dzeboev^a, and I. V. Losev^{a,c}

Received April 30, 2020; revised May 3, 2020; accepted May 5, 2020

Abstract—The paper presents the results of GNSS observations, provided by the authors in 2010–2019 years, in the zone of contact of tectonic structures of the Siberian platform, West-Siberian plate and West-Sayan orogenic area. We presented the first time assessment of the velocities of modern horizontal movements and the structural-kinematic model of block movements in a southern sector of the Yenisei Ridge. This model enables to assess the geodynamic safety of disposal of high-level radioactive waste in granite gneisses rocks of the Nizhne-Kansk massif.

Keywords: modern horizontal crustal movements, Siberian Platform, West Siberian Plate, Lower Kan massif, GNSS observations, radioactive waste

DOI: 10.1134/S1028334X20070077

The southern part of the Yenisei Ridge is located at the junction of large regional tectonic structures, namely, the ancient Siberian Platform, the epi-Hercynian West Siberian Plate, and the West Sayan orogenic fold zone [1]. Within the boundaries of the Nizhne-Kansk granite–gneiss massif, which directly borders on the Atamanovskiy branch of the Yenisei Ridge, the building of an underground research laboratory (URL) for validating the safety of disposal of high-level radioactive waste (RAW) began in 2019 [2].

In 2010, researchers of the Mining and Chemical Combine at Zheleznogorsk and the Geophysical Center, Russian Academy of Sciences, organized a satellite geodetic network within the boundaries of the Nizhne-Kansk massif; this network included 30 GNSS stations intended for observations of modern crustal movements (MCMs) [3]. Seven observation cycles were carried out using this network, and the time series obtained for the period from 2010 to 2019 reflecting changes in the coordinates of GNSS stations were analyzed.

To determine the displacement vectors and deformation rates, we used the methods and algorithms

described in [4, 5]. The basis for processing of the GNSS data and their interpretation were base-line vectors and their correlation matrices obtained from statistical processing and diagnostic equalizing of the measurements cycles conducted from 2010 to 2019. We obtained the time series of displacements for 23 geodetic stations. Table 1 provides the calculated displacement velocity for the GNSS stations presented in Fig. 1 (the velocities are calculated for the first time). The root mean square (RMS) errors in determination of their plan-view position for particular measurement epochs did not exceed 3–3.5 mm [5].

When designing the geodynamic polygon, the structural–tectonic scheme of the region was used [6], according to which the field of MCMs is determined by geodynamic interaction between the largest tectonic structures of the West Siberian Plate and the Siberian Platform (Fig. 1), which border each other along the Muratovskiy fault and subordinate faults, mainly of submeridional direction [7].

The map of the velocities of MCMs was analyzed together with the first-class highly accurate leveling data [8] and the data of geological surveys [9]. Figure 2 shows the field of average annual velocities of horizontal MCMs and the result of their kinematic interpretation. The study area is subdivided into 13 large structural blocks, separated in most cases by large tectonic faults identified earlier from geological data [6, 10].

The obtained velocities of horizontal MCMs (Table 1) indicate the contemporary tectonic activity of the Muratovskiy, Atamanovskiy, Kansko-Atamanovskiy, Pravoberezhnyi, and Shumikhinskiy faults

^a Geophysical Center, Russian Academy of Sciences, Moscow, 119296 Russia

^b Schmidt Institute of Physics of the Earth, Russian Academy of Sciences, Moscow, 123995 Russia

^c Mining Institute, National University of Science and Technology MISiS, Moscow, 125009 Russia

*e-mail: a.manevich@gcras.ru

Table 1. Velocities of horizontal MCMs in the eastern (v_e) and northern (v_n) directions for 2012–2019 and RMS errors in their determination (σ_e and σ_n , respectively)

Codes of GNSS stations	Measurement interval	Mean movement velocity v_e , mm/yr	Mean movement velocity v_n , mm/yr	RMS error for σ_e , mm	RMS errors for σ_n , mm
1205	2012–2019	–0.15	–1.42	0.90	1.05
1206	2012–2019	0.05	0.96	0.81	0.99
1214	2012–2019	–1.49	–0.26	0.95	1.17
1215	2012–2019	–0.53	–0.23	0.99	1.28
1216	2012–2019	–0.02	1.35	0.96	1.19
LP04	2012–2019	–1.56	–0.91	0.80	1.00
LP05	2012–2019	0.01	–0.93	0.97	1.20
LP06	2012–2019	–0.22	–1.13	1.25	1.58
LP07	2012–2019	1.15	2.35	0.89	1.10
OPO2	2012–2019	–0.80	0.21	0.84	1.06
OPO3	2012–2019	0.65	–0.11	1.05	1.30
1209	2014–2019	1.18	0.53	0.84	0.59
1219	2014–2019	–0.27	–1.92	0.71	0.50
1401	2014–2019	0.13	1.73	0.82	0.58
1201	2012–2016	0.17	–0.32	1.09	1.35
1202	2012–2016	0.41	2.37	0.66	0.80
1204	2012–2016	–3.83	0.21	0.46	0.56
1207	2012–2016	0.79	1.33	0.63	0.88
1211	2012–2016	0.71	–2.87	1.54	2.10
1212	2012–2016	0.85	–1.38	1.28	1.56
1213	2012–2016	–2.15	–0.36	0.59	0.72
LP08	2012–2016	1.02	–1.11	0.49	0.63
LP09	2012–2016	3.68	1.23	0.48	0.63

(Figs. 1, 2). Within the West Siberian Plate, the velocities of movement show a quite uniform distribution; three blocks with maximum velocities of $\sim 2\text{--}3$ mm/yr have been distinguished here (Fig. 2).

Movements in the central and northern part of the zone contact between the West Siberian Plate and the Siberian Platform (structural blocks IV and V) change direction from sublatitudinal to submeridional, indicating strike–slip motions along the Muratovskiy and Atamanovskiy faults (Fig. 2). This segment is the most mobile in the study area. The structural blocks VI, VIII, IX, X, and XI, confined by the Kansko-Atamanovskiy fault to the north and by the Muratovskiy fault to the west, demonstrate the highest movement gradients with the velocities of up to 3.5 mm/yr.

Block movements along the Pravoberezhnyi strike-slip fault have produced a bench rock structure. Notably the maximum gradients of horizontal MCMs have been obtained at the contact between blocks VII and IX. The change in horizontal motions from sublatitudinal to submeridional match with the Shumikha fault, which across the URL construction site (rectan-

gle in Fig. 2). This structural block is located at a distance of 2–3 km from the contact zone between the West Siberian Plate and the Siberian Platform and, undoubtedly, is affected by motions along this boundary.

The model obtained is consistent with the results of structural–geological and geodynamic studies in the area [6–8, 10]. The velocity of approach of the Siberian Platform and the West Siberian Plate in their interaction zone within the southern Yenisei Ridge can be estimated at 2–4 mm/yr. Notably, the velocity of motion of the West Siberian Plate is lower than that of the Siberian Platform by 1–2 mm/yr. This probably caused uplift of the Atamanovskiy branch at the neotectonics stage, when the ancient Siberian Platform and the young West Siberian Plate were hypsometrically separated. The Siberian Platform was uplifted to absolute altitudes of $\sim 700\text{--}800$ m, while the West Siberian Plate appeared to be relatively lowered by 120–200 m [7]. The Atamanovskiy Range has been ascending since at least the Quaternary, as is indicated by the inherited character of motions [7]. As a result of

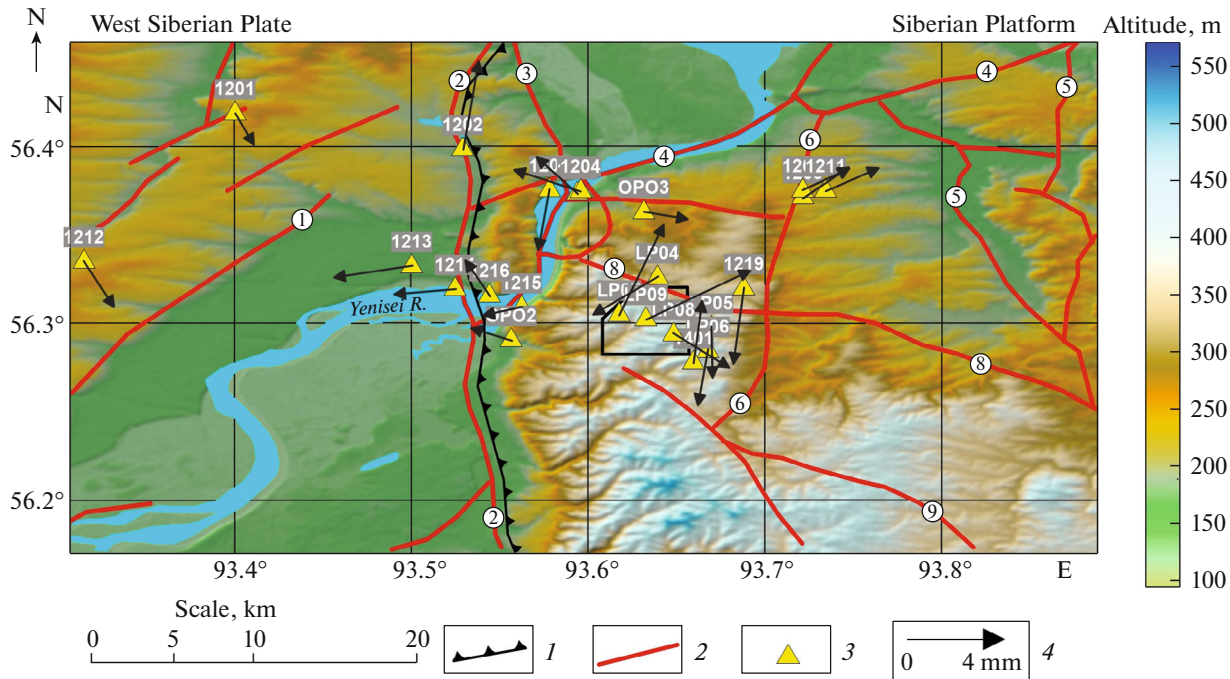


Fig. 1. Structural–tectonic scheme and modern horizontal movements in the southern Yenisei Ridge: (1) boundary between the Siberian Platform and the West Siberian Plate; (2) large tectonic faults; (3) GNSS stations; (4) vectors of velocities of MCMs at GNSS stations, mm/yr. Encircled Arabic numerals here denote the main tectonic faults: 1, First Krasnoyarskiy; 2, Muratovski; 3, Atamanovski; 4, Kansko-Atamanovski; 5, Malotel'ski; 6, Pravoberezhny; 7, Bol'shetel'ski; 8, Shumikhinski; 9, Baykal'skiy.. The rectangle denotes the URL construction site.

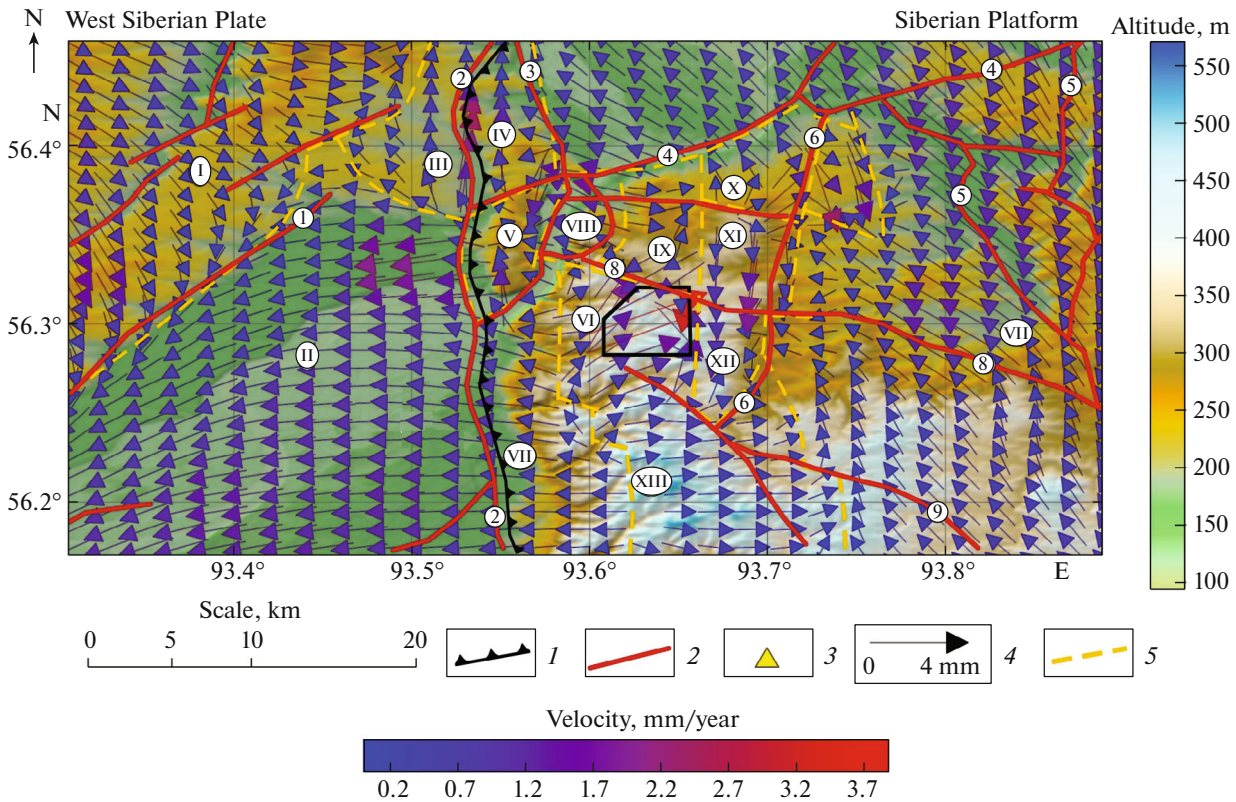


Fig. 2. Average velocities field of horizontal MCMs in the southern Yenisei Ridge: (1) boundary between the Siberian Platform and the West Siberian Plate; (2) large tectonic faults; (3) GNSS stations; (4) vectors of velocities of MCMs, mm/yr; (5) active geodynamic zones corresponding to the boundaries between structural blocks possessing different kinematics. Arabic numerals denote the main faults (see Fig. 1). Latin numerals denote tectonic blocks revealed from GNSS observations.

this, block VII moves westwards and block XIII moves eastwards.

Additionally, the cyclicity in the development of geodynamic motions has been revealed in the geodynamic research area [3]. In 2013–2014, activation of the geodynamic regime was recorded: it was manifested in the form of a change in the deformation sign for both compression and extension on the western and eastern banks of the Yenisei River.

In general, it can be thought that the regional movements are caused by sublatitudinal compression along the azimuth of $\sim 100^\circ$ – 110° . The velocities of horizontal MCMs obtained within the tectonic blocks are relatively low, which confirms the stable geodynamic regime of the structural block where the URL site is located. Thus, the results of the present work demonstrate the possibility of high-level RAW disposal within this structural block.

ACKNOWLEDGMENTS

In this work we used the instrumentation and data provided by the core facilities center (Analytical Center of Geomagnetic Data, Geophysical Center, Russian Academy of Sciences; <http://ckp.gcras.ru/>).

FUNDING

This study was supported by the Russian Science Foundation (project no. 18–17–00241 entitled “Study of rock massif stability by system analysis of geodynamic processes for geocologically safe underground of radioactive waste isolation”).

REFERENCES

1. V. A. Vernikovskiy, D. V. Metelkin, A. E. Vernikovskaya, et al., *Russ. Geol. Geophys.* **57** (1), 46–68 (2016).
2. N. P. Laverov, V. I. Velichkin, B. T. Kochkin, V. I. Mal'kovskii, V. A. Petrov, and A. A. Pek, *Geokol. Inzh. Geol., Gidrogeol., Geokriol.*, No. 3, 195–206 (2010).
3. V. N. Tatarinov, V. N. Morozov, V. I. Kaftan, and A. I. Manevich, *Geofiz. Issl.* **19** (4), 64–79 (2018).
4. A. D. Gvishiani, V. I. Kaftan, R. I. Krasnoperov, V. N. Tatarinov, and E. V. Vavilin, *Izv., Phys. Solid Earth* **55** (1), 33–50 (2019).
5. V. I. Kaftan, A. D. Gvishiani, V. N. Morozov, and V. N. Tatarinov, *Sovr. Probl. Distant. Zondir. Zemli Kosmosa*, No. **1**, 83–94 (2019).
<https://doi.org/10.21046/2070-7401-2019-16-83-94>
6. R. M. Lobatskaya, *Russ. Geol. Geophys.* **46** (2), 138–147 (2005).
7. S. V. Belov, V. N. Morozov, V. N. Tatarinov, E. N. Kamnev, and J. Hummer, *Geokol. Inzh. Geol., Gidrogeol., Geokriol.*, No. 3, 248–266 (2007).
8. P. P. Kolmogorova and V. G. Kolmogorov, *Russ. Geol. Geophys.* **45** (4), 421–429 (2004).
9. O. A. Morozov, A. V. Rastorguev, and G. D. Neuvazhaev, *Radioakt. Otkhody*, No. **4**(9), 46–62 (2019).
<https://doi.org/10.25283/2587-9707-2019-4-46-62>
10. D. M. Bachmanov, A. I. Kozhurin, and V. G. Trifonov, *Geodin. Tektonofiz.* **8** (4), 711–736 (2017).
<https://doi.org/10.5800/GT-2017-8-4-0314>

Translated by N. Astafiev